Asymmetric Split-Vacancy Defects in SiC Polytypes: A Combined Theoretical and Electron Spin Resonance Study

Viktor Ivady, Andreas Gällström, Nguyen Son Tien, Erik Janzén and Adam Gali

Original Publication:

Viktor Ivady, Andreas Gällström, Nguyen Son Tien, Erik Janzén and Adam Gali, Asymmetric Split-Vacancy Defects in SiC Polytypes: A Combined Theoretical and Electron Spin Resonance Study, 2011, Physical Review Letters, (107), 19, 195501.
http://dx.doi.org/10.1103/PhysRevLett.107.195501

Asymmetric Split-Vacancy Defects in SiC Polytypes: A Combined Theoretical and Electron Spin Resonance Study

Viktor Ivády,[1] Andreas Gällström,[2] Nguyen Tien Son,[2] Erik Janzén,[2] and Adam Gali[1,3,*]

[1]*Research Institute for Solid State Physics and Optics of the Hungarian Academy of Sciences, PO Box 49, H-1525, Budapest, Hungary*
[2]*Department of Physics, Chemistry and Biology, Linköping University, SE-581 83 Linköping, Sweden*
[3]*Department of Atomic Physics, Budapest University of Technology and Economics, Budafoki út 8, H-1111 Budapest, Hungary*

(Received 28 August 2011; published 2 November 2011)

Transition metal defects were studied in different polytypes of silicon carbide (SiC) by *ab initio* supercell calculations. We found asymmetric split-vacancy (ASV) complexes for these defects that preferentially form at only one site in hexagonal polytypes, and they may not be detectable at all in cubic polytype. Electron spin resonance study demonstrates the existence of ASV complex in niobium doped 4*H* polytype of SiC.

DOI: 10.1103/PhysRevLett.107.195501 PACS numbers: 61.72.J−, 61.82.Fk, 71.15.Mb, 76.30.−v

Polytypism is a special case of polymorphism where the two-dimensional translations within the layers are essentially preserved in a crystal. Polytypism has attracted growing interest in materials science among group IV [1–3] and group III-V [4–8] semiconductors. Recent efforts have been made to explore the electrical and optical properties of different polytypes of pristine crystals [9–12]. However, relatively little is known about the complexity of point defects that may appear in different polytypes of a given crystal, which significantly influence their electrical and optical properties. As an illustrative example, we discuss briefly the case of a single substitutional defect and a vacancy-pair complex in silicon carbide (SiC) polytypes where SiC is a prototype material for polytypism and many forms can be relatively easily fabricated.

SiC is a typical semiconductor with tetrahedral bonds between Si and C atoms. The basal plane consists of a hexagonal lattice. Depending on the stacking sequences of Si-C bilayers perpendicular to the basal plane, one can build cubic (3*C*), hexagonal (typically 4*H* and 6*H*), or rhombohedral SiC polytypes. 3*C* SiC contains 3 Si-C bilayers in its unit cell with all cubic (*k*) stacking sequences. 4*H*- and 6*H*-SiC polytypes contain 4 and 6 bilayers in their primitive cell with cubic and hexagonal (*h*) stacking sequences such as *hkhk* in 4*H* and $hk_1k_2hk_1k_2$ in 6*H* where the positions of the atoms in the third neighbor of the cubic k_1 and k_2 sites are different [see Fig. 1(a)]. If *N* atom substitutes one C atom in these SiC crystals (N_C defect) then two *inequivalent* substitutional sites will appear in 4*H* SiC whereas three sites will appear in 6*H* SiC. Correspondingly, one may assume that two (three) N_C-related signals are expected in 4*H* (6*H*) SiC. Indeed, one, two, and three ionization energies are associated with N_C in 3*C*, 4*H*, and 6*H* SiC, respectively [13]. The complexity of pair defects is even more pronounced than that of a single substitutional defect. For instance, divacancy, comprised of adjacent carbon and silicon vacancies, could have four possible configurations (e.g., *h*-*k*, *k*-*h*, *h*-*h*, *k*-*k*) in 4*H* SiC whereas there are six possible configurations in 6*H* SiC. Indeed, electron spin resonance (ESR) studies found 4 and 6 signals associated with divacancy in hexagonal polytypes (see Ref. [14] and references therein). According to these examples, a general rule may be invoked in the study of signals coming from unidentified defects in polytypic semiconductors that the number of signals should be equal to the number of possible configurations at inequivalent sites for substitutional or vacancy defects. This assumption *a priori* indicates that the formation energies are about the same for a given point defect (i) in different polytypes and (ii) at inequivalent sites within a polytype of a given crystal.

We report *ab initio* study on six transition metal (*M*) defects in 3*C*-, 4*H*-, and 6*H*-SiC polytypes. We found that there is a class of *M* defects that preferentially substitutes the Si site (M_{Si}). However, there is another class of *M* defects that can form a special asymmetric split-vacancy configuration in hexagonal SiC polytypes. The asymmetric split-vacancy defect is similar to the M_{Si}-C_{vac} complex where C_{vac} labels C vacancy. We show that *h*-*h* configuration of these M_{Si}-C_{vac} defects in hexagonal polytypes are much more stable than any other pair configurations. As a consequence, only one signal among the possible four and six configurations of M_{Si}-C_{vac} defects is expected in 4*H* and 6*H* hexagonal polytypes, respectively, while M_{Si}-C_{vac} defects have much lower concentration than the M_{Si} defect in cubic 3*C* polytype, and may not be detectable at all. The existence of an asymmetric split-vacancy defect is demonstrated by our ESR study on niobium doped 4*H* SiC. Our finding clearly indicates that (i) the relative stability of defects in between different polytypes may significantly change and that (ii) complex substitutional or vacancy defects may have very different stability among the possible configurations provided by the number of inequivalent sites in a given polytype. Furthermore, this proves that some point defects will preferentially form in hexagonal polytypes that may be absent in cubic polytype.

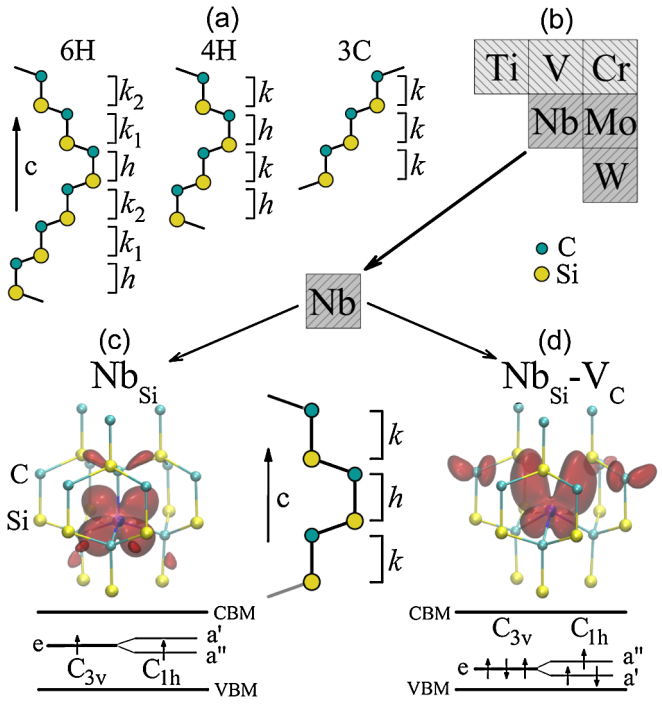

FIG. 1 (color online). (a) Unit cells and notation of Si-C bilayers in 6*H*, 4*H*, and 3*C* SiC polytypes. (b) The fraction of periodic table with the elements considered in our study. Light gray shaded impurities are preferentially Si substitutionals in any polytypes (c), while dark gray shaded impurities may also form a complex with C vacancy resulting in an asymmetric split-vacancy configuration in hexagonal polytypes (d). (c),(d) The geometry of neutral niobium impurity at *h* and *h*-*h* configurations in 4*H* SiC, respectively, where the lobes represent the isosurface of the calculated spin density with a value of 0.014. Schematic diagram of the electronic structure in the band gap is also depicted. CBM (VBM) is conduction (valence) band edge. Neutral niobium is Jahn-Teller unstable with reducing the symmetry.

We used the density functional theory (DFT) based Vienna *ab initio* simulation package (VASP) [15] with the projector augmented-wave (PAW) method [16] and plane-wave basis set. In the case of metals we utilized small core PAW projectors. We applied plane-wave cutoff of 420 eV with Γ-point sampling of the Brillouin zone in 512-atom 3*C*-SiC, 576-atom 4*H*-SiC, and 432-atom 6*H*-SiC supercells. In these large supercells the Γ-point calculations provide convergent charge and spin densities and simultaneously allow us to monitor the degeneracy of the defect levels in the fundamental band gap. We applied both semilocal Perdew-Burke-Ernzerhof (PBE) [17] and nonlocal Heyd-Scuseria-Ernzerhof (HSE06) [18,19] functionals in the calculations where the latter heals the band gap error of the PBE functional [20]. The defects were optimized in the supercell until all forces fell below 10 meV/Å in all cases. We calculated the adiabatic charge transition levels as explained in Ref. [21].

We studied titanium (Ti), vanadium (V), niobium (Nb), chromium (Cr), molybdenum (Mo), and tungsten (W) impurities in 3*C*, 4*H*, and 6*H* polytypes of SiC. The motivation of this selection was twofold: (i) experimental data were available for most of these impurities in SiC [13,22,23], which made a comparison between theory and experiment possible, (ii) the trends could be studied among $4s^2 3d^2$-$3d^4$ *M* defects and among $4s^2 3d^4$-$6s^2 5d^4$ *M* defects (see Fig. 1). We refer only to these six selected impurities as *M* defects in the rest of this Letter. We found that the interstitial and carbon substituting *M* defects have very high formation energies in any SiC polytypes and will not be considered further. Two configurations have the lowest formation energies: (i) *M* impurity substitutes Si, M_{Si}, in other words, occupies Si vacancy, (ii) M_{Si} forms a complex with C vacancy, in other words, *M* impurity occupies divacancy. A schematic diagram of the relative stabilities and defect structures is shown in Fig. 1.

It is instructive to discuss the electronic structure of M_{Si} and M_{Si}-C_{vac} defects before providing their calculated geometries and formation energies because the formation energy may depend on stoichiometry of SiC and the charge state of the defect provided by the actual position of the Fermi level [24]. The early first row M_{Si} defects were already analyzed in Ref. [25] where local density approximation was applied with a scissor operator in 3*C*- and 4*H*-SiC polytypes. We briefly give the main finding: the *d* states of *M* impurity will split in T_d and C_{3v} crystal fields of 3*C* and hexagonal polytypes, respectively. In the case of 3*C* SiC the five *d* orbitals split as t_2 and *e* levels where the t_2 level will recombine with the C sp^3 dangling bonds while the *e* level remains atomiclike. This *e* level will be filled by 0, 1, 2 electrons when *M* = Ti, V, Cr, respectively. The position of the *e* level tends to lie closer to the valence band edge (E_{V}) which gets occupied. In hexagonal polytypes we gave a detailed group theory analysis for the case of $\mathrm{Mo_{Si}}$ [22], which is basically valid for the first row M_{Si} defects with taking into account the occupation of the 3*d* orbital: in that case the five *d* orbitals will split as $\{a_1, e(1)\}$ and $e(2)$ orbitals where $\{a_1, e(1)\}$ is similar to the t_2 state in 3*C* SiC, but the slight mixture between $e(1)$ and $e(2)$ is allowed by symmetry. Generally, high spin states are the ground state of M_{Si} defects because the Hund rule is valid for degenerate atomiclike orbitals. For instance, the $e(2)$ level is occupied by two electrons with parallel spins resulting in an $S = 1$ state for neutral Cr, Mo, W, and negatively charged V, Nb substituting the Si site.

It is important to notice that the states originated from strongly localized *d* orbitals may be not well described by the semilocal PBE functional that was partially discussed in Ref. [25]. According to our HSE06 calculation, the position of the fully occupied $e(2)$ level in the spin-up channel ($S = 1$, $M_S = 1$) will shift down with respect to E_{V} by about 1.0, 0.3, 0.1 eV compared to PBE values for *M* = Cr, Mo, W, respectively, whereas the gap "opens" by

0.93 eV. The defect states are qualitatively well described by the PBE functional; however, a gap correction is needed for calculation of charge transition levels, and the $e(2)$ level is not pinned to E_V.

The calculated energy difference between cubic and h sites of M_{Si} defects is within 0.1 eV for any M impurity in any charge state in hexagonal polytypes. This result was obtained by both PBE and HSE06 functionals. This small energy difference (i) indicates that the concentration of M_{Si} defects is about the same, so 2 (3) signals are expected for M_{Si} defects in 4H (6H) polytypes, (ii) allows us to discuss the possible charge states of the defects only at the h site in hexagonal polytypes. According to the aforementioned analysis, Ti may be negatively charged, and V, Nb, Cr, Mo, and W may be positively or negatively charged by filling or emptying the $e(2)$ level. In this Letter we focus on the conditions of the formation of these defects. SiC is usually grown by chemical vapor deposition (CVD), high temperature CVD (HTCVD), or physical vapor transport (PVT), which may be considered as a quasiequilibrium process at relatively high temperatures (1600–1900 K in CVD and above 2300 K in HTCVD and PVT) where the Fermi level tends to lie close to midgap. If M impurities were introduced into SiC by implantation, then many defects would be created that compensate the sample; thus, the quasi-Fermi level is also set close to midgap. The stochiometry of SiC samples depends on the growth parameters; C vacancy is often present in HTCVD and PVT SiC samples confirmed by ESR [26]. All in all, we consider the formation energy of M_{Si} and M_{Si}-C_{vac} defects where the Fermi level is not far from midgap and in Si-rich condition.

Next, we describe the M_{Si}-C_{vac} complex. As can be seen in Fig. 1(d) this complex is rather a split-vacancy defect where the M impurity sits in divacancy. In this compound semiconductor the M impurity is not exactly in the middle of divacancy but stays closer to the Si vacancy by about 0.4 Å than to C vacancy, forming an asymmetric split-vacancy (ASV) configuration. Symmetric split-vacancy configuration is very well known in homopolar semiconductors possessing D_{3d} symmetry [27]. However, the highest symmetry of ASV defects is C_{3v} in heteropolar 3C SiC, and at the axial configurations in hexagonal polytypes, whereas the symmetry is reduced to C_{1h} at basal configurations. We analyze the C_{3v} symmetry configuration by invoking the defect-molecule picture and group theory. In divacancy the silicon and carbon dangling bonds create two a_1 and two e states where the highest energy of the e state is localized on the silicon dangling bonds (C vacancy). The s orbital of the M impurity transforms as a_1 while the d orbitals split to one a_1 and two e states. The a_1 states of the divacancy and M impurity can recombine as well the corresponding e states resulting in a_1, a_1, e, and e bonding states and the corresponding antibonding combinations. If we take $M[s^2d^4]$ impurity with 6 valence electrons and the 6 valence electrons in divacancy, then 12 electrons occupy these states. That means that all the bonding orbitals are fully occupied, resulting in a singlet ground state of $a_1^{(2)}a_1^{(2)}e^{(4)}e^{(4)}$. According to our calculations the last e defect state appears in the fundamental gap. In short, neutral Ti($e^{(2)}$) has $S = 1$, neutral V and Nb($e^{(3)}$) have $S = 1/2$, whereas neutral Cr, Mo, and W($e^{(4)}$) have $S = 0$ ground state in ASV configurations. As a consequence, Ti, V, Nb may be positively and negatively ionized by emptying or filling this e state, while Cr, Mo, and W can be definitely positively ionized in ASV defects. We found antibonding a_1^*, e^* levels in the fundamental gap of hexagonal polytypes for these defects as well, so they can also be negatively ionized. We calculated the defects in all of these charge states. Briefly, these defects will be either neutral or negatively ionized in hexagonal polytypes under experimental conditions of formation.

The formation energies of the most stable h-h ASV configurations are compared with M_{Si} defects in 4H SiC in Fig. 2. The results are the same within 0.1 eV in 6H polytypes. Apparently, the formation energies of ASV complexes are comparable to simple M_{Si} defects for M = Nb, Mo, W impurities in hexagonal polytypes. This means that ASV complexes may form with similar concentration as M_{Si} defects in hexagonal polytypes. This is particularly true for the Si-rich condition where many C vacancies are formed. According to our calculations, ASV has extremely high stability for M = Nb, Mo, W impurities where the binding energy between M_{Si} and C_{vac} is over 4 eV. This also means that diffusing C_{vac}, that is mobile at typical growth temperature, is trapped very effectively by these M impurities. In the case of M = Ti, V, Cr, M_{Si} is definitely preferred. Indeed, 2 (3) photoluminescence, deep level transient spectroscopy and ESR signals were found associated with these M impurities in 4H (6H) SiC [13,28] that can be explained by the number of inequivalent substitutional sites in these polytypes, while only a single ESR line was observed for Mo [28] and W [29] in 6H SiC. We note here that the PBE functional makes ASV defects much more preferable. The reason is that the atomiclike e state of M_{Si} shifts down with a considerable amount in HSE06 calculation with respect to PBE calculation while the e state of ASV defects is heavily mixed with the Si dangling bonds, so they are pinned to E_V. As a consequence, the formation energy difference increases in HSE06 calculations with respect to PBE calculations. This sheds light on the importance of using nonlocal DFT functionals when relative stabilities of transition metal defects are studied in semiconductors.

Moreover, we found that h-h configurations of ASV defects are much more stable than any other combinations involving cubic sites in hexagonal polytypes for M = Nb, Cr, Mo, W. The next stable configuration is $M(h)$-$C_{vac}(k)$ with an energy difference of more than 0.6 eV, at least among these M impurities. The reason for the exclusive site selection is due to the comfortable

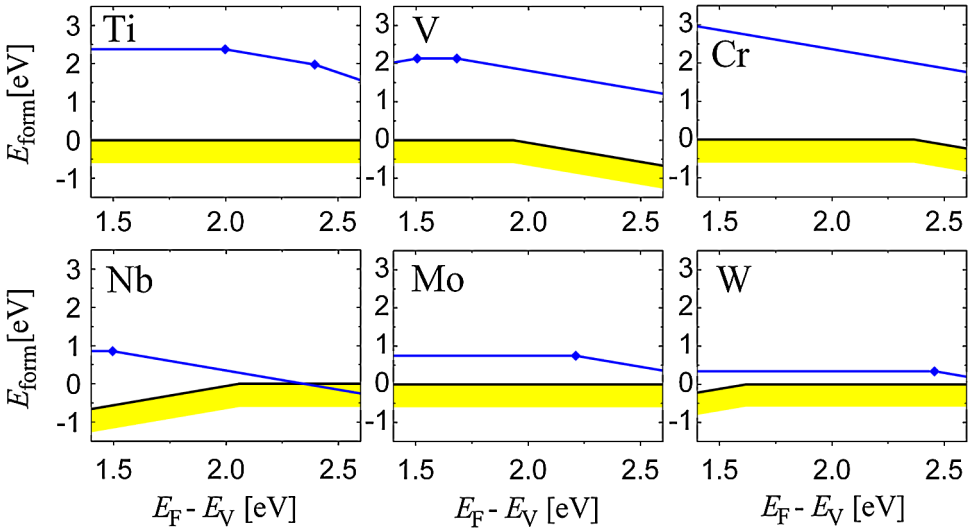

FIG. 2 (color online). The relative formation energies between M_{Si} (black line) and M_{Si}-C_{vac} [gray (blue) line] defects at h sites in 4H SiC as a function of the position of the Fermi level with respect to valence band edge ($E_F - E_V$) calculated by HSE06 functional. We aligned the reference formation energy to that of the neutral M_{Si} defects. The formation energy of M_{Si} defects are shown for Si-rich condition. The bottom of the shaded area corresponds to that for C-rich condition.

situation of the $\{d_{xy}, d_{xz}\}$ and $\{d_{yz}, d_{x^2}\}$ orbitals which can only maximally overlap with Si dangling bonds of C_{vac} if first neighbor Si atoms of C_{vac} are placed just above the first neighbor C atom of the M impurity [see Fig. 1(d)]. In any other configuration of C_{vac}, the d states have to "twist" in order to form a molecular orbital with Si dangling bonds. As a consequence, the corresponding e defect state lies deeper in the gap for h-h configuration than for other configurations, lowering its formation energy. We note that the k-k configuration is, at least, more than 1.0 eV less stable than h-h configuration in hexagonal polytypes. This explains our finding in cubic polytype: M_{Si} defects are much more stable than ASV defects for any M impurity.

Finally, we demonstrate the existence of ASV defects in 4H SiC by ESR study. We chose Nb impurity for which the existence of ASV configuration is most likely among M defects according to our calculations (see Fig. 2). The 4H SiC samples used in this study were grown by high-temperature CVD in a reactor with several parts made of NbC. The samples are semi-insulating and the concentration of unintentionally incorporated Nb is $\sim 3 \times 10^{16}$ cm^{-3} as determined by secondary ion mass spectrometry. We found only one Nb-related ESR spectrum with a clear hyperfine (hf) structure consisting of 10 equal-intensity lines characteristic for a hf interaction with one ^{93}Nb atom (see Fig. 3). The defect shows C_{1h} symmetry with $S = 1/2$ spin state. Beside the main ESR line of Nb, hf signals of two symmetrically equivalent Si atoms are detected. Analyzing the observed angular dependences of the ^{93}Nb and ^{29}Si hf lines using the spin Hamiltonian $H = \mu_B \mathbf{BgS} + \mathbf{SA}^{Nb}\mathbf{I}_{Nb} + \mathbf{SA}^{Si}\mathbf{I}_{Si}$ (here $S = 1/2$, $I_{Nb} = 9/2$, $I_{Si} = 1/2$), we obtain the principal values $g_{xx} = 1.9891$, $g_{yy} = 2.1080$, $g_{zz} = 2.0272$ (for the g tensor), $A_{xx} = 73.7$, $A_{yy} = 16.0$, $A_{zz} = 30.7$ (for the ^{93}Nb hf A^{Nb} tensor), and $A_{xx} = 55.1$, $A_{yy} = 40.9$, $A_{zz} = 41.5$ (for the ^{29}Si hf A^{Si} tensor). Here the principal A values are measured in units of 10^4 cm^{-1} and the angles between the principal z axis of the g or A tensors and the c axis are 17.2° for the g tensor, 28.4° for the A^{Nb} tensor, and 0° for the A^{Si} tensor. From the obtained ^{93}Nb and ^{29}Si hf tensors, spin localizations on Nb ($\sim$ 40.3%) and two Si neighbors ($\sim$ 30.3%) were estimated, indicating considerable localization of spin density on two Si atoms near Nb impurity. According to the theory, only the neutral Nb_{Si} or Nb_{Si}-C_{vac} ASV defects may have $S = 1/2$ spin state. In these cases, the appropriate e level of Nb_{Si} is occupied by one electron while it is occupied by three electrons in the Nb_{Si}-C_{vac} ASV complex. Both cases are the subject of Jahn-Teller distortion with reducing the symmetry from C_{3v} to C_{1h}, which is pronounced for the ASV complex where the d

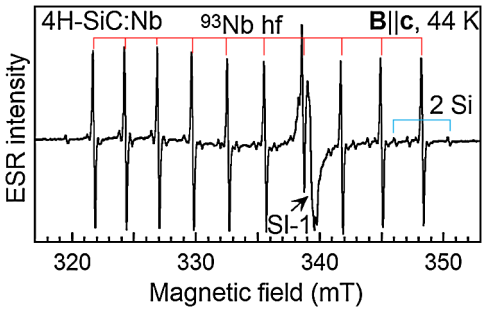

FIG. 3 (color online). ESR spectrum observed in Nb-doped 4H SiC in darkness at 44 K for $\mathbf{B} \parallel c$, showing the hyperfine structures of one ^{93}Nb and two equivalent ^{29}Si. The broad line at $\sim$339.26 mT is the isotropic signal of the SI-1 defect (Ref. [30]).

orbitals are mixed with Si dangling bonds of C_{vac}. The spin density distribution is significantly different between Nb_{Si} and Nb_{Si}-C_{vac} [see Figs. 1(c) and 1(d)]. In Nb_{Si}, it is localized almost entirely on the *d* orbitals of Nb whereas it is considerably mixed with two Si dangling bonds in Nb_{Si}-C_{vac}. This excludes Nb_{Si} as the origin of our Nb-related ESR signal while it strongly implies the ASV model. The calculated formation energies explain why only a single Nb-related signal was measured in the 4*H* polytype of SiC. Our preliminary ESR study of Nb-doped 6*H* SiC also shows only one Nb-related spectrum with C_{1h} symmetry that further supports our conclusion.

In summary, we proposed for some transition metal impurities that asymmetric split-vacancy defects can form in hexagonal polytypes of SiC that are stable only at *h*-*h* configuration. ESR studies confirmed this proposal for niobium impurity. Our finding indicates that some electrically and optically active defects may appear in hexagonal polytypes that are absent in cubic polytype, and the number of signals may not follow the number of possible configurations in a given polytype.

Support from the Swedish Foundation for Strategic Research, the Swedish Research Council, the Swedish Energy Agency, the Swedish National Infrastructure for Computing Grants No. SNIC 011/04-8 and No. SNIC001-10-223, and the Knut and Alice Wallenberg Foundation is acknowledged.

*agali@eik.bme.hu

[1] Y. Lifshitz, X. F. Duan, N. G. Shang, Q. Li, L. Wan, I. Bello, and S. T. Lee, Nature (London) **412**, 404 (2001).
[2] C. Raffy, J. Furthmüller, and F. Bechstedt, Phys. Rev. B **66**, 075201 (2002).
[3] F. J. Lopez, E. R. Hemesath, and L. J. Lauhon, Nano Lett. **9**, 2774 (2009).
[4] M. I. McMahon and R. J. Nelmes, Phys. Rev. Lett. **95**, 215505 (2005).
[5] V. G. Dubrovskii and N. V. Sibirev, Phys. Rev. B **77**, 035414 (2008).
[6] M. Heiss, S. Conesa-Boj, J. Ren, H.-H. Tseng, A. Gali, A. Rudolph, E. Uccelli, F. Peiró, J. R. Morante, D. Schuh, E. Reiger, E. Kaxiras, J. Arbiol, and A. Fontcuberta i Morral, Phys. Rev. B **83**, 045303 (2011).
[7] C. Thelander, P. Caroff, S. Plissard, A. W. Dey, and K. A. Dick, Nano Lett. **11**, 2424 (2011).
[8] D. Kriegner, C. Panse, B. Mandl, K. A. Dick, M. Keplinger, J. M. Persson, P. Caroff, D. Ercolani, L. Sorba, F. Bechstedt, J. Stangl, and G. Bauer, Nano Lett. **11**, 1483 (2011).
[9] B. Wen, J. Zhao, M. J. Bucknum, P. Yao, and T. Li, Diam. Relat. Mater. **17**, 356 (2008).
[10] B. D. Malone, J. D. Sau, and M. L. Cohen, Phys. Rev. B **78**, 035210 (2008).
[11] A. De and C. E. Pryor, Phys. Rev. B **81**, 155210 (2010).
[12] T. Ito, T. Kondo, T. Akiyama, and K. Nakamura, J. Cryst. Growth **318**, 141 (2011).
[13] *Recent Major Advances in SiC*, edited by W. J. Choyke, H. Matsunami, and G. Pensl (Springer-Verlag, Berlin, 2004).
[14] N. T. Son, P. Carlsson, J. ul Hassan, E. Janzén, T. Umeda, J. Isoya, A. Gali, M. Bockstedte, N. Morishita, T. Ohshima, and H. Itoh, Phys. Rev. Lett. **96**, 055501 (2006).
[15] G. Kresse and J. Furthmüller, Phys. Rev. B **54**, 11 169 (1996).
[16] P. E. Blöchl, Phys. Rev. B **50**, 17 953 (1994).
[17] J. P. Perdew, K. Burke, and M. Ernzerhof, Phys. Rev. Lett. **77**, 3865 (1996).
[18] J. Heyd, G. E. Scuseria, and M. Ernzerhof, J. Chem. Phys. **118**, 8207 (2003).
[19] A. V. Krukau, O. A. Vydrov, A. F. Izmaylov, and G. E. Scuseria, J. Chem. Phys. **125**, 224106 (2006).
[20] M. Marsman, J. Paier, A. Stroppa, and G. Kresse, J. Phys. Condens. Matter **20**, 064201 (2008).
[21] P. Deák, B. Aradi, T. Frauenheim, E. Janzén, and A. Gali, Phys. Rev. B **81**, 153203 (2010).
[22] A. Gällström, B. Magnusson, and E. Janzén, Mater. Sci. Forum **615–617**, 405 (2009).
[23] F. C. Beyer, C. G. Hemmingsson, A. Gällström, S. Leone, H. Pedersen, A. Henry, and E. Janzén, Appl. Phys. Lett. **98**, 152104 (2011).
[24] B. Aradi, A. Gali, P. Deák, J. E. Lowther, N. T. Son, E. Janzén, and W. J. Choyke, Phys. Rev. B **63**, 245202 (2001).
[25] M. S. Miao and W. R. L. Lambrecht, Phys. Rev. B **74**, 235218 (2006).
[26] N. T. Son, P. Carlsson, J. ul Hassan, B. Magnusson, and E. Janzén, Phys. Rev. B **75**, 155204 (2007).
[27] G. D. Watkins, Phys. Rev. B **12**, 4383 (1975).
[28] J. Baur, M. Kunzer, and J. Schneider, Phys. Status Solidi A **162**, 153 (1997).
[29] K. Irmscher, I. Pintilie, L. Pintilie, and D. Schulz, Physica (Amsterdam) **308–310B**, 730 (2001).
[30] N. T. Son, B. Magnusson, Z. Zolnai, A. Ellison, and E. Janzén, Mater. Sci. Forum **457–460**, 437 (2004).